SEMARAK ILMU PUBLISHING

Journal of XX

Journal homepage:
https://semarakilmu.com.my/journals/
ISSN: XXXX-XXXX

UNVEILING THE INFLUENCE OF ALUMINIUM INCORPORATION ON THE STRUCTURAL, OPTICAL, AND MAGNETIC CHARACTERISTICS OF GD-DOPED ZNO

Nur Amaliyana Raship[1], Siti Nooraya Mohd Tawil[1,2*], Khadijah Ismail[2], and Nafarizal Nayan[3]

[1] Centre for Tropicalisation, Defence Research Institute, Universiti Pertahanan Nasional Malaysia (UPNM), Kem Sungai Besi 57000, Kuala Lumpur, Malaysia
[2] Department of Electrical and Electronic Engineering, Universiti Pertahanan Nasional Malaysia (UPNM), Kem Sungai Besi 57000, Kuala Lumpur, Malaysia
[3] Microelectronic and Nanotechnology-Shamsuddin Research Centre (MiNT-SRC), Universiti Tun Hussein Onn Malaysia (UTHM), 86400 Parit Raja, Batu Pahat, Johor, Malaysia

ARTICLE INFO

Article history:

Keywords:
Gd; Rare-earth; ZnO; Co-sputtering; AFM; MFM

ABSTRACT

This paper presents the properties of ZnO thin films enhanced by the incorporation of Gd (3 at%) and Al (3 at%), which were synthesized using a simultaneous target sputtered onto glass substrate. Using X-ray diffractometer, the crystalline structure of the films was determined showing the effective incorporation both doping elements into ZnO lattice. This has been proved as no secondary phases or any peaks associated to Gd and Al in the deposited films. EDS results further demonstrated the presence of Gd and Al ions within films with amount of concentration were 3 at% for each respective element. The surface morphology exhibited homogenous nanoparticles structure for all the deposited films in which the nanoparticle size became smaller as Gd and Al were added to ZnO films. The optical properties by UV-Vis showed good transmittance that surpassing 90 % of average transmittance for all the films. The bandgap obtained using Tauc's plot equation based on the transmittance results were increased when both Gd and Al were incorporated. The magnetic properties of the co-doping films were obtained using magnetic force microscopy (MFM). The results showed that the MFM images for the film incorporating Gd and Al had a bright-dark contrast as compared to the undoped one. It further unveils improved magnetic properties, as evidence by its larger value of δf_{rms}. Based on these findings, adding 3 at% of Al to the Gd-doped ZnO films has further enhanced its physical, optical and magnetic characteristics, which in turn could also improve its magnetic behaviour at room temperature.

1. Introduction

In the past few years, zinc oxide (ZnO) have been relied as a semiconductor host material considering its advantageous properties, which include a significant exciton binding energy of 60 meV and direct band gap energy of 3.37 eV [1]. ZnO additionally exhibits exceptional electrical and optical characteristics, which have led to many commercial applications, especially in spintronics [2], solar cells [3], photocatalytic [4],[5],[6], and sensors [7]. However, the disadvantage of ZnO is that the materials nature is non-magnetic, which restricts their use in spintronic devices. In this respect, magnetic ions particularly, transition metal (TM) ions or rare earth (RE) ions has been

extensively research as a dopant element to tune the characteristics of host materials like ZnO and GaN materials [8],[9] providing new possibilities for spintronic applications. Among both of magnetic ions (TM and RE), doping with RE ions has attracted much interest since it present high magnetism at room temperature [10],[11]. Gadolinium as dopant magnetic ions is vital element due to their unique magnetic contributions, ionic radii, valence states, and coordination numbers, that induces high magnetic moments [11]. Doping of Gd additionally boost the conductive properties of holes in ZnO, as holes in the Gd 4*f* orbitals are more energetic instead of electrons [12]. Additionally, compared to other rare earth elements, it has a higher optical bandgap of 5.3 eV, which improves optical transparency by allowing light to be emitted at a longer wavelength and absorbed at a shorter wavelength [13].

At the present time, research is being done on co-doping the ZnO-based DMS system with Group II, III, and IV elements to further enhance its physical, optical, electrical and magnetic properties. Group III elements, in particular, including Al [14],[15], and Ga [16],[17] are among the primary dopants used as donors for promotion of the properties of ZnO-based DMS films especially in optical, electrical and magnetic characteristics. Al prevails over competing Group III elements owing to their low ionic radii (0.054 nm) as opposed to Zn (0.074 nm) and Gd (0.094 nm), allowing easy incorporation in ZnO-based DMS films. Several studied have proved that doping of Al^{3+} elements, which have one extra valence electrons makes ZnO films more conductive because of extra carriers brought into the material [18]. Some have also reported that extra carriers from Al doping could extend the ferromagnetism of the ZnO-based DMS films [19],[20],[21]. Thus, we anticipate that the combination of excellent properties of co-doping (Gd, Al) can tailor the properties of ZnO, potentially unlocking whole new properties for advanced technological applications, particularly in spintronics. Although other research has employed a variety of synthesis methods, including co-precipitation [22],[23],[24], spin coating [25], hydrothermal [26], and MBE [27], the co-sputtering method for co-doping Gd and Al ions into ZnO concurrently is still not well-studied in the literature. In the present work, we employed co-sputtering technique to deposit undoped ZnO, Gd-doped ZnO, and (Gd, Al) co-doped ZnO films. Our aim is to investigate the role of Al in Gd-doped ZnO and compare its properties to those of undoped ZnO and Gd-doped ZnO films.

2. Methodology

A comparative study is carried out between ZnO films that are undoped, ZnO films that are doped with 3 at% of Gd, and ZnO films that are co-doped with 3 at% of (Gd, Al) utilizing the co-sputtering technique. Different target materials consists of ZnO, Gd, and Al were initially placed in the sputtering chamber. The glass substrate on which the film is deposited is also positioned in the chamber. The sputtering procedure then begins with the introduction of inert gas, typically argon gas to ignite the plasma. The sputtering process, then continues with the sputtering power set 0 W to Gd and Al target for undoped ZnO. The sputtering power for the Gd target was set to 75 W for the Gd-doped ZnO film. In the case of (Gd, Al) co-doped ZnO, the sputtering power was set to 75 W and 15 W for Gd and Al targets, respectively. A working pressure of 5 mTorr of working pressure and deposition time of 1 hour were used for the deposition process. The parameters for depositing all the films are listed in Table 1. More information on the deposition process to prepare all of the films were provided in our preceding publication [28].

Table 1
List of fixed and variable parameters for the deposition process

Parameter	Value
Base pressure	7.0×10^{-6} Torr
Working pressure	10 mTorr
Argon flow rate	29 sccm
Time deposition	60 minutes
Distance target to substrate	13.5 cm
Sputtering power	100 W
Rotating substrate holder	9 rpm
Film concentration	Undoped ZnO, Gd-doped ZnO (3 at%), (Gd, Al) co-doped ZnO (3 at%)

A series of characterization techniques, which include X-ray diffraction (XRD), field emission scanning electron microscopy (FESEM), energy dispersive X-ray spectroscopy (EDS), ultra-violet visible spectroscopy (UV-Vis), and magnetic force microcopy used to investigate the properties of the deposited films. The PANalytical X'pert Pro, X-ray equipment equipped with a Cu Kα source, was used for assessing the structural properties of the film. Scan speed and step size for the samples were 5°/min and 0.03° in the 2θ range, which covers 20° to 80°. The film's surface morphology was investigated with the FESEM (JEOL JSM-7600F). To determine the elements and the atomic percentage (at %) in the deposited films, EDS analysis was employed in addition to probing the instrument to FESEM. The optical transmittance in the 300–1000 nm wavelength region was measured using a Shimadzu UV 1800 ultraviolet–visible spectrophotometer. The magnetic domain structures of the films were thoroughly analyzed at an area of 1 μm × 1 μm and a lift-scan height of 50 nm using MFM in tapping mode. Every measurement was done at room temperature.

3. Results and Discussion

3.1 *Structural Properties*

Figure 1 shows the patterns of X-ray diffraction of all films produced on glass substrates, namely undoped ZnO, Gd-doped ZnO, and (Gd, Al) co-doped ZnO. The XRD data presents two diffraction peaks, which belong to the planes of (002) and (103) with (002) planes being the dominant. These peaks are located at 2θ of 34.2° and 62.75°, which demonstrates the formation of ZnO hexagonal wurtzite structure verified by JCSD No. 98-018-6243. Despite doping together with Gd and Al, no additional phases or peaks linked with these elements were detected in the XRD pattern. This proves the effective replacement of Zn ions in the ZnO lattice by Gd and Al ions [29]. As ZnO is co-doped with Gd and Al, the originally strong and intense diffraction peaks grew broader and weaker. This indicates that dopant films have a poor crystalline structure, which Gd and Al ion doping decreases ZnO crystallinity. Furthermore, the films doped with Gd and (Gd, Al) showed a displacement of the diffraction peaks towards a lower diffraction angle. The peak shift is produced by differences in the ionic radius of Zn (0.074 nm), Gd (0.094 nm), and Al (0.054 nm) due to the presence of both Gd and Al on the ZnO structure [5],[30].

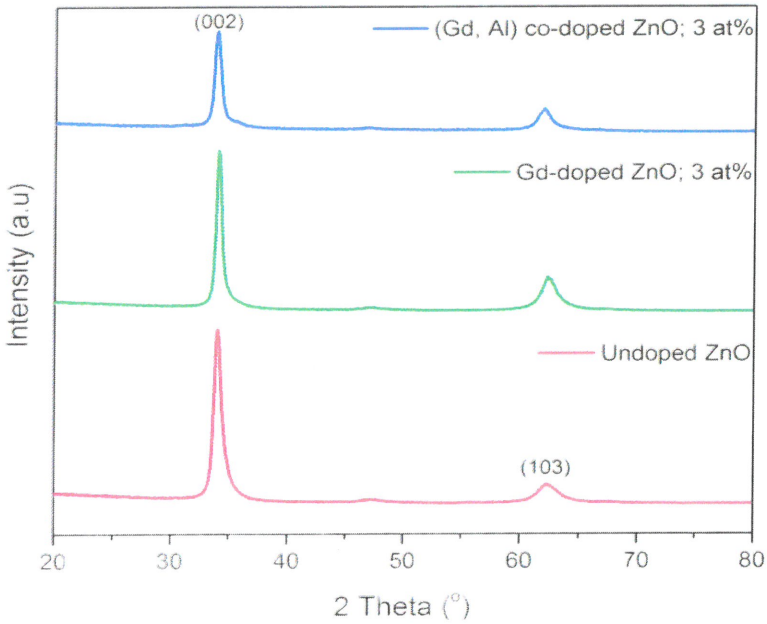

Fig. 1. XRD patterns of undoped ZnO, Gd-doped ZnO, and (Gd, Al) co-doped ZnO films

3.2 Morphological Properties

The morphology of the synthesized films was assessed using FESEM, and the resulting images are presented in Figure 2.

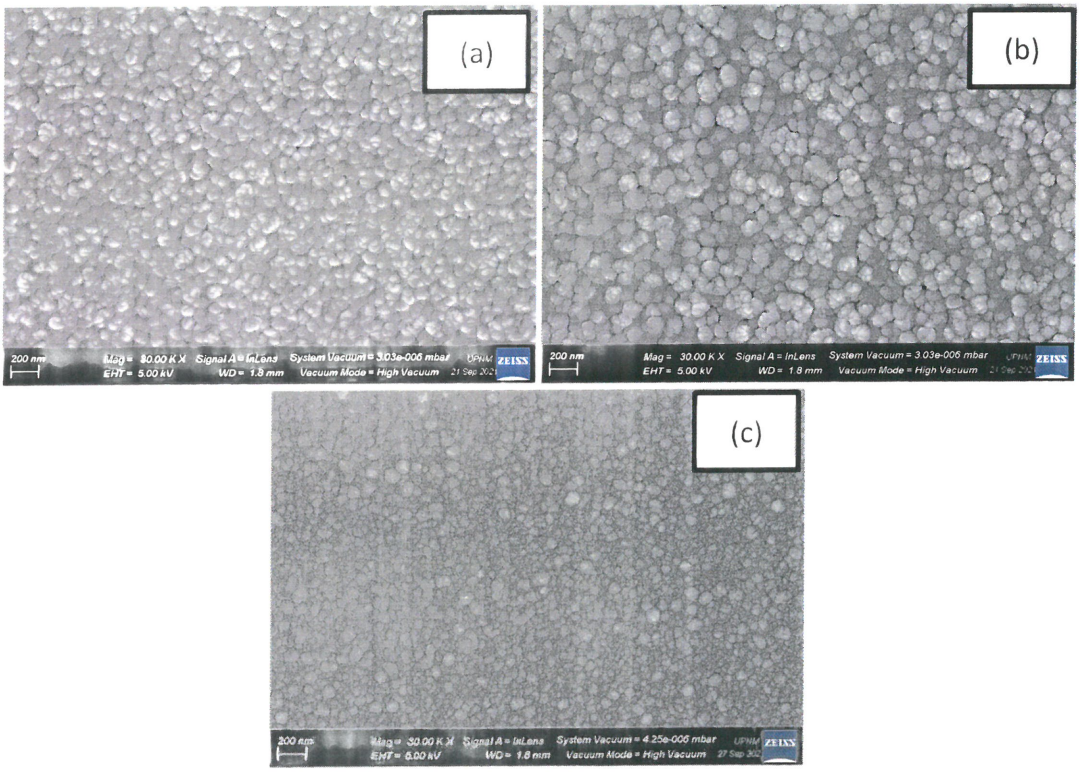

Fig. 2. FESEM images of (a) undoped ZnO, (b) Gd-doped ZnO, and (c) (Gd, Al) co-doped ZnO films

The synthesized undoped ZnO, Gd-doped ZnO and (Gd, Al) co-doped ZnO showed a spherical morphology with a homogeneous particle structure, as confirmed by FESEM images. As observed in FESEM images, the surface morphology remains unchanged despite the addition of Gd and (Gd, Al) doping. However, the spherical morphology has fewer boundaries and more finer as Gd and Al incorporated into ZnO. The size of the particle structure also decreases after doping ZnO with Gd and Al as displayed in Figure 2(c). This can be explained by dopant elements that fill the gaps in the ZnO structure and cause a reduction in the average size of spherical shapes, thus producing smaller structures [31]. Similar observations are also previously reported [29],[32]. These results are interconnected with the XRD analysis as the addition of Gd and Al into ZnO modify the dimensional properties of the crystal lattice and cause disruptions, leading to broadening and reducing crystallinity which in turn impact the size and shape of the ZnO particles. Overall, the smaller grains are expected to be helpful for spin-based electronics because they lessening the occurrence of magnetic domain boundaries, improving the material's magnetic homogeneity.

Figure 3 shows the EDS spectrum obtained from EDS analysis, which was used to examine the elemental distribution and atom presence in undoped ZnO, Gd-doped ZnO, and (Gd, Al) co-doped ZnO films.

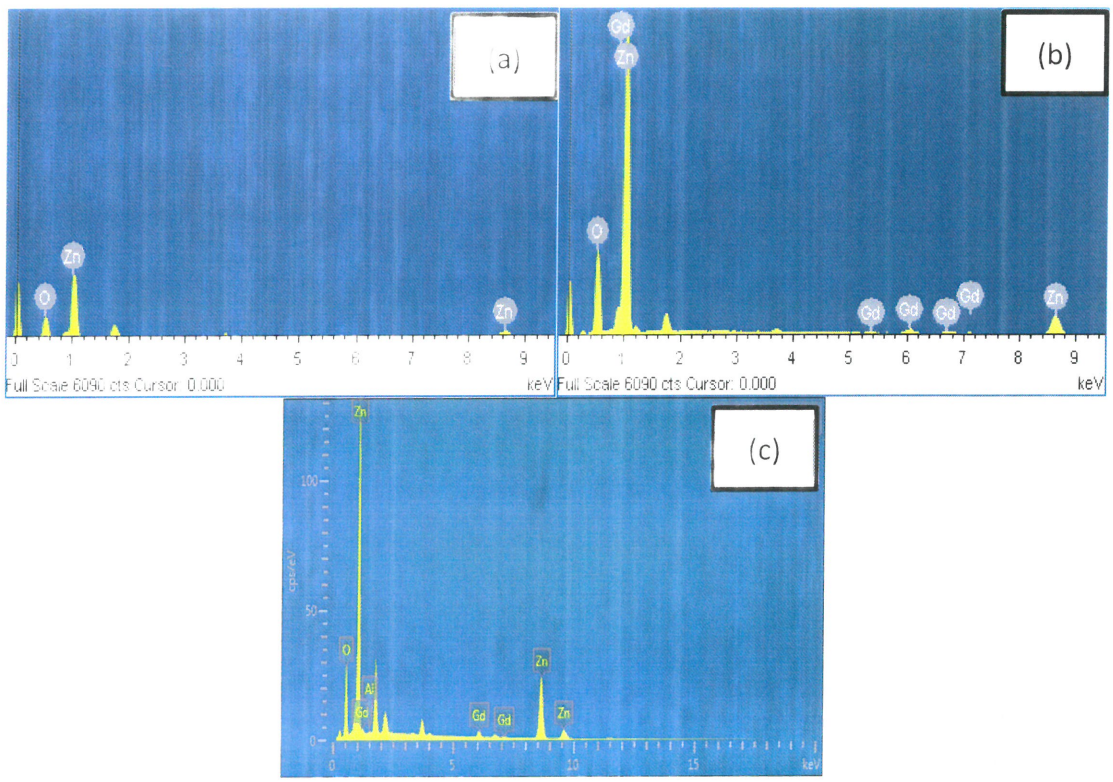

Fig. 3. EDS spectrum of (a) undoped ZnO, (b) Gd-doped ZnO, and (c) (Gd, Al) co-doped ZnO films

According to the EDS spectrum of undoped ZnO film in Figure 3(a), Zn is the most prevalent element, followed by O. Figure 3(b), depicts the existence characteristics element of Gd, Zn, and O in EDS spectrum for Gd-doped ZnO films, revealing that Gd atoms were successfully doped [5]. The EDS spectrum revealed the presence of an extra element Al peak in the ZnO co-doped with Gd and Al (Figure 3(c)), in addition to Zn, O, and Gd elements, confirming both dopant elements were fully incorporated into ZnO. It should be noted that despite the different selected areas of the measured film that were chosen, all of the films had consistent

element content, demonstrating the uniform and continuous distribution of Zn, O, Al, and Gd in deposited films. Table 2 list the results of the atomic percentage for each element presents in all films. These findings reveal that all the films are free of impurities and other elements except Gd, Al, Zn, and O.

Table 2
Atomic percentage (at%) of each element in the prepared films

Sample	Zn (%at)	O (at%)	Al (at%)	Gd (at%)
Undoped ZnO	38.92	61.08	NA	NA
Gd-doped ZnO	37.58	59.33	NA	3.09
(Gd, Al) co-doped ZnO	41.80	52.14	3.06	3.00

3.3 Optical Properties

The transmittance spectra of ZnO films that are undoped, Gd-doped, and co-doped with Al and Gd are provided in Figure 4(a). The films were all tested at room temperature within the wavelength range of 300 nm to 1000 nm. All synthesized films possess good transparency in the visible spectrum, with an average transmittance rises above 90 %. The (Gd, Al) co-doped ZnO film exhibited the highest transmittance spectra, indicating that co-doped (Gd, Al) into ZnO improves the transparency of the film. The obtained results is consistent with the smaller grains and finer structure exhibited in FESEM images as the fine structure reduced scattering of light, contributing to higher transparency in (Gd, Al) co-doped ZnO film. The absorption edge is termed as the wavelength at which the percentage transmission is zero seen to shift slightly to lower wavelength with Gd doping and (Gd, Al) co-doping as exhibited in Figure 4(b). This blue shift in transmittance occurs due to material modifications, where different dopants ions (Gd, Al) have replaced the Zn ions [33].

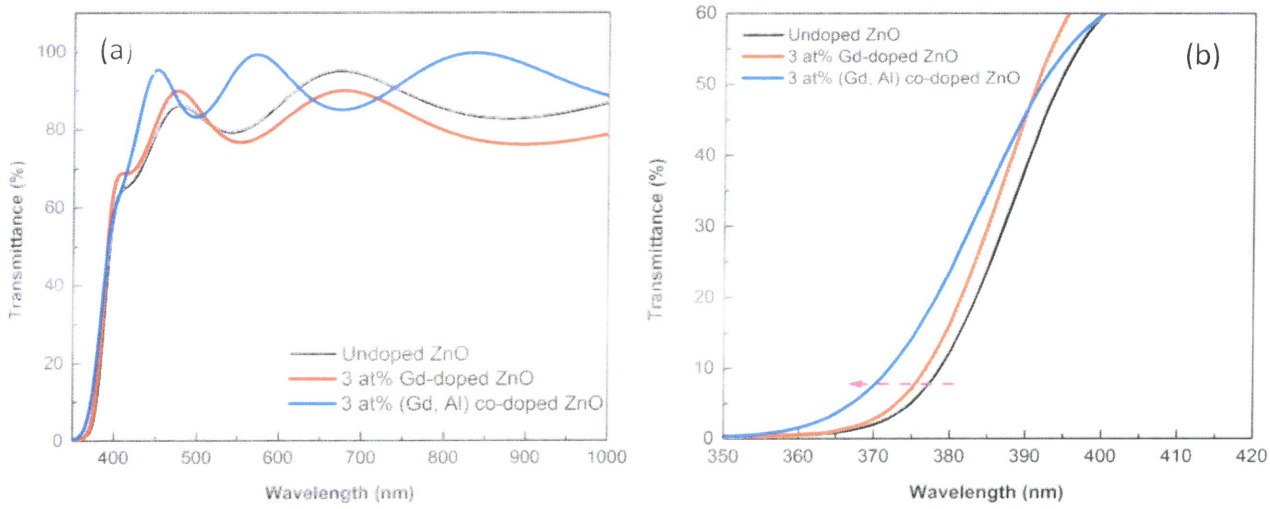

Fig. 4. (a) Transmittance spectra, and (b) Absorption edge of undoped ZnO and doped films

The bandgap for each film was measured through extrapolating of the straight-line from a graph of $(\alpha h\nu)^2$ against $h\nu$, predicted by the equation of Tauc. Figure 5(a) to 5(c) presents the graph plotted for undoped ZnO, and doped films. Based on the presented graph, the estimated bandgap of undoped ZnO film was 3.09 eV. By incorporating Gd and (Gd, Al), the bandgap value increased to

3.10 eV and 3.15 eV, respectively. The comparison value of bandgap energy for all the films were tabulated in Table 3. This broadening in bandgap was caused by the Moss-Burstein phenomenon [34]. The interaction of ions Zn^{2+} and O^{-} in undoped ZnO films resulting in deficiency of free charge carriers. By substituting Zn^{2+} ions with Gd^{3+} and Al^{3+} ions in the ZnO lattice, additional free electrons are introduced into the valence band. Since the donor electrons from Gd^{3+} and Al^{3+} occupy the bottom states in the conduction band, electrons in the valence band need extra energy to transition into higher conduction band states. For this reason, the edge of the absorption band moving upward towards high photon energy and widens the bandgap. Thus, broadening in bandgap by co-doping with Al helps in improving the spin polarization of charge carriers, which is critical in spintronic devices especially for their spin detection and spin injection [35].

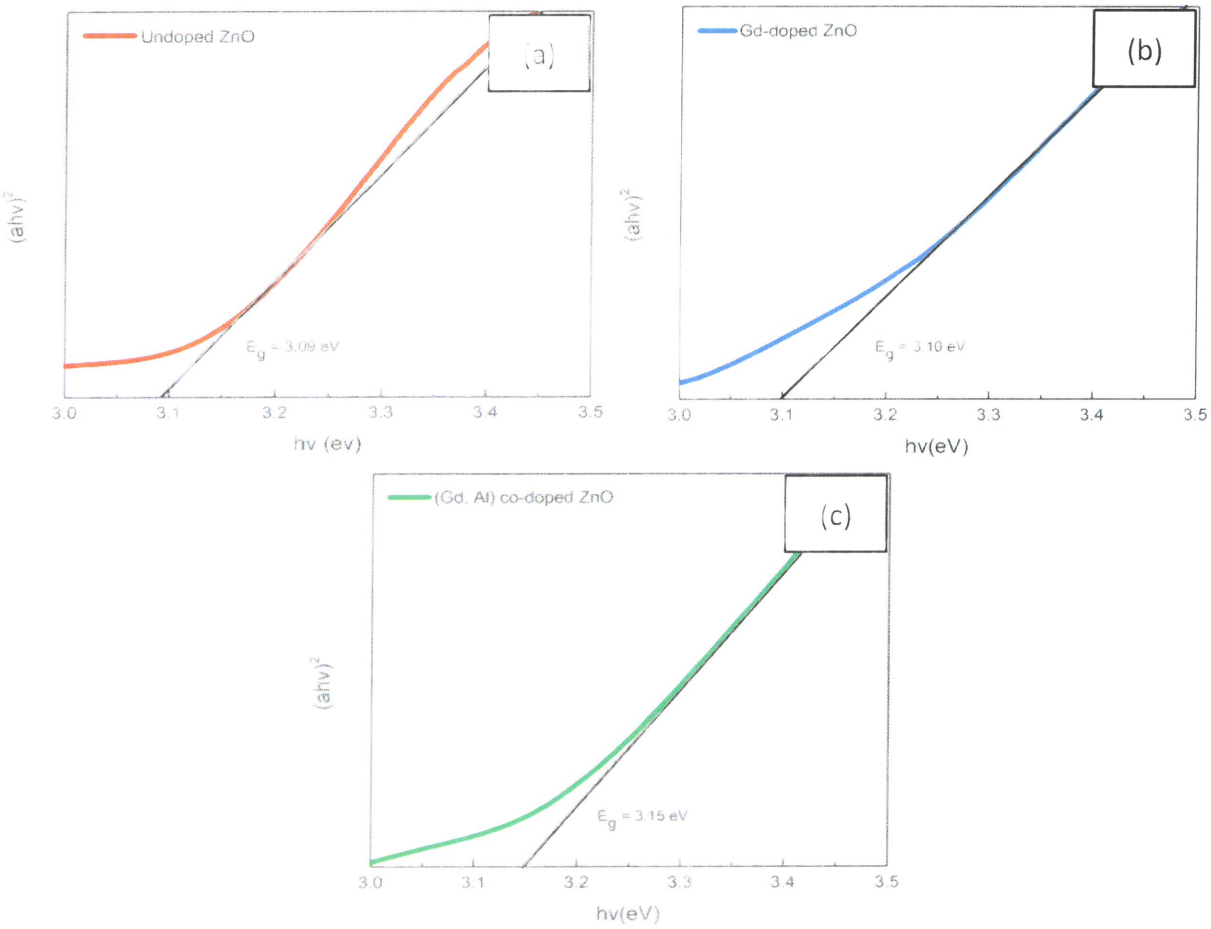

Fig. 5. Linear plot projection of band gap energy of (a) Undoped ZnO, (b) Gd-doped ZnO, and (c) (Gd, Al) co-doped ZnO films

Table 3
Value of bandgap energy for all prepared films

Sample	Bandgap energy (eV)
Undoped ZnO	3.09
Gd-doped ZnO	3.10
(Gd, Al) co-doped ZnO	3.15

3.4 Magnetic Properties

The MFM analysis was performed to measure the magnetic characteristics; the MFM images yielded information on magnetic features, including the root mean square value of frequency shift (δf_{rms}). MFM measures the magnetic structure of the film surface by scanning magnetic samples with magnetic probes and monitoring the interaction between the probes and surfaces. The equation below used to express the magnetic force operating between the tip and the sample [36]:

$$F = \mu_0 \int \nabla (M_{tip} \cdot H_{sample})\, dV_{tip} = \mu_0 \int \nabla (M_{sample} \cdot H_{tip})\, dV_{sample} \quad (1)$$

where, M_{tip} and M_{sample} represents the tip's convolution and the sample magnetic moment, respectively meanwhile, H_{tip} and H_{sample} represented by the tip and sample stray magnetic field, respectively. There are two forces that are acting on the magnetic tip as it moves across the sample's surface, which are repulsive and attractive forces. The interactions of spin polarization in parallel (N, N) and (N), which the tip and films resemble to the repulsive forces, while the opposite (S, N) and (N) refer to the attractive forces. The domain magnetic structure pattern is described by the bright-dark contrast apparent in MFM images, which correlates to the (S) and (N) magnetic poles' spin polarisation [37], [38].

In Figure 6, the left side displays two-dimensional (2D) AFM topography images, while the right side displays 2D MFM images of undoped ZnO, and doped films. The topography and corresponding MFM images were captured for each film, with scanning size of 1 µm x 1 µm and a fixed 50 nm lift tip distance. Figure 6(a) displays that undoped ZnO exhibits no visible phase contrast, indicating an extremely weak magnetic response. This result is predictable since the undoped ZnO film is non-magnetic material, thus no magnetic signal is shown. Subsequently, with similar scanning circumstances, singly doped (Gd) and co-doped (Gd, Al) films exhibit an obvious magnetic response, as observed in Figure 6(b) and 6(c). The bright-dark contrast was clearly shown within the MFM images, suggesting the signs of magnetism in doped films [38]. The δf_{rms} were estimated from the MFM image of all synthesized films using XEI software as tabulated in Table 4. The δf_{rms} is characterized as average magnitude of magnetic variations within the scanned area of the MFM images. The analysis revealed that the δf_{rms} of undoped ZnO, Gd-doped ZnO, and (Gd, Al) co-doped ZnO films were 0.12, 0.69, and 9.10, accordingly. The results of δf_{rms} increased when singly doped with Gd and continuously improved when co-doped with (Gd, Al). A higher δf_{rms} value indicates stronger magnetic interactions between the probe and the scanning film, which forming a high magnetic contrast [39]. This result suggests that Al as co-dopant significantly change the crystal growth, with enhanced morphology and structure quality, contributing to the improvement of the magnetic behavior reflected by the high value of δf_{rms}.

Table 4
Value of δf_{rms} for all prepared films

Sample	δf_{rms}
Undoped ZnO	0.12
Gd-doped ZnO	0.69
(Gd, Al) co-doped ZnO	9.10

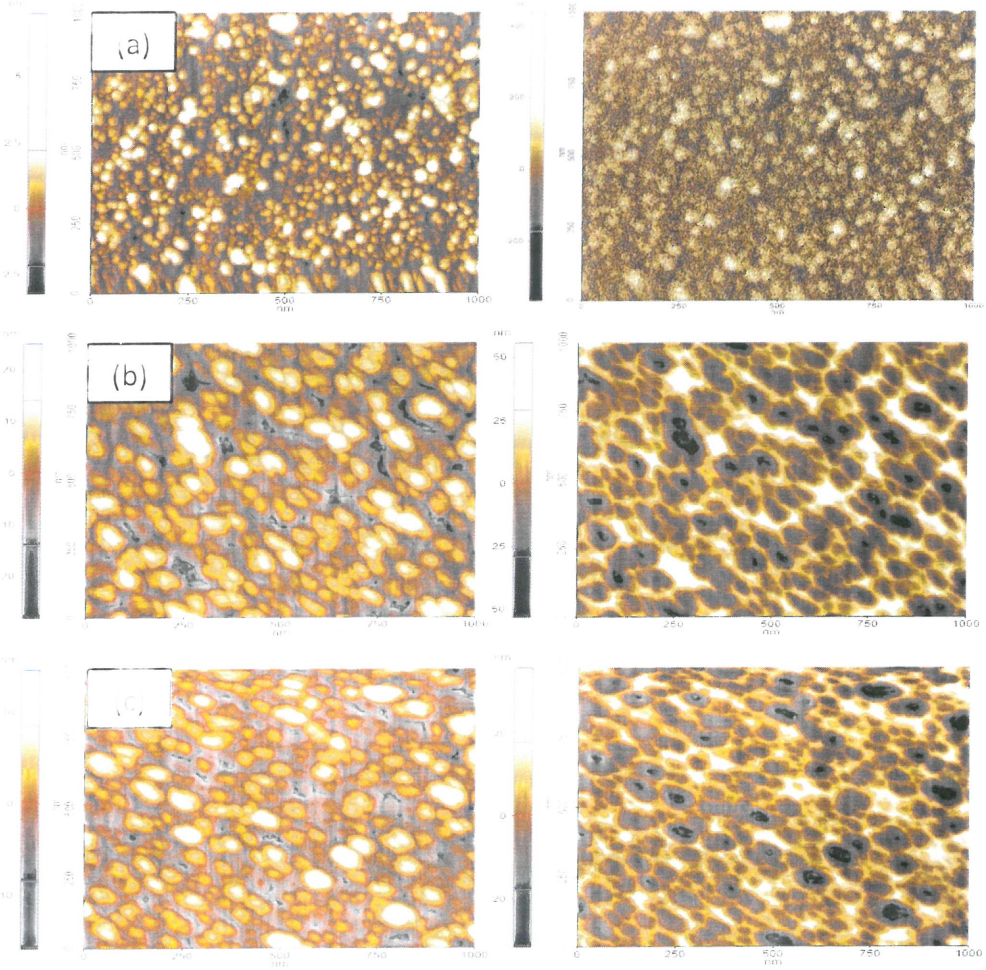

Fig. 6. (Right) 2D MFM images, and (left) 2D AFM images, of (a) Undoped ZnO, (b) Gd-doped ZnO, and (c) (Gd, Al) co-doped ZnO films

4. Conclusions

Three different films namely undoped ZnO, Gd-doped ZnO and (Gd, Al) co-doped ZnO have been successfully synthesized using co-sputtering method. XRD, FESEM, EDS, UV-Vis, and MFM were used to characterize the films and explore all their properties. The structural, morphological, optical, and magnetic characteristics are strongly impacted by the Al co-doping. The XRD analysis found a pure phase of hexagonal wurtzite in ZnO, despite ZnO being singly doped and co-doped (Gd, Al), as no different peaks appear in the XRD pattern. The crystallinity of the films, however, declined after Al co-doping into ZnO. The substitution of Gd and Al led to modification of the crystal lattice, results in decrease of particle's size with more refined structure. The incorporation of doping elements was confirmed through EDS spectrum, which identified an appearance of only Gd, Al, O, and Zn peak. The films with co-doping of Al exhibited better transparency, with bandgap was blue-shifted opposed to the undoped ZnO film. MFM measurements show the enhanced ferromagnetism in doping films with improved magnetic behavior upon co-doped of (Gd, Al), as evident by their larger δf_{rms} value. Overall, film with Al as co-dopant contributes to structural and morphological refinement, high transparency, broader bandgap and

enhanced magnetic properties. Hence, ZnO films co-doped with 3 at% (Gd, Al) can be concluded as an optimum film with excellent properties, which benefit for spintronic applications.

Acknowledgement

The authors express their gratitude to Microelectronics and Nanotechnology Shamsudin Research Centre (MiNT-SRC), Universiti Tun Hussein Onn Malaysia for help extended during the research. We are also grateful for the funding provided by the Grant UPNM/2024/GPPP/TK/1 from Universiti Pertahanan Nasional Malaysia.

References

[1] Dhirendra Kumar Sharma, Sweta Shukla, Kapil Kumar Sharma, and Vipin Kumar. 2020. "A Review on ZnO: Fundamental Properties and Applications." Materials Today: Proceedings 49(8): 3028–35. https://doi.org/10.1016/j.matpr.2020.10.238.

[2] Fazal Kabir, Adil Murtaza, Azhar Saeed, Awais Ghani, Anwar Ali, Saleh Khan, Kaili Li. 2022. "Structural, Optical and Magnetic Behavior of (Fe, Te) Co-Doped ZnO Based Dilute Magnetic Semiconducting Nanocrystals." Ceramics International 48 (14): 19606–17. https://doi.org/10.1016/j.ceramint.2022.03.095

[3] Khuili, M., N. Fazouan, H. Abou El Makarim, E. H. Atmani, D. P. Rai, and M. Houmad. 2020. "First-Principles Calculations of Rare Earth (RE=Tm, Yb, Ce) Doped ZnO: Structural, Optoelectronic, Magnetic, and Electrical Properties." Vacuum 181 (April): 109603. https://doi.org/10.1016/j.vacuum.2020.109603.

[4] Dash, Debasrita, and Dojalisa Sahu. 2022. "Growth and Gd Doping of ZnO Nanostructures with Enhanced Structural, Optical Properties and Photocatalytic Applications." IOP Conference Series: Materials Science and Engineering 1219 (1): 012037. https://doi.org/10.1088/1757-899x/1219/1/012037.

[5] Chanu, L. Anju, K. Jugeshwar Singh, and K. Nomita Devi. 2023. "Intrinsic Defect Enhanced Photocatalytic Activity of Gd^{3+} Doped ZnO Nanoparticles." Materials Chemistry and Physics 303 (February): 127832. https://doi.org/10.1016/j.matchemphys.2023.127832.

[6] Marinho, Juliane Z., Leonardo F. de Paula, Elson Longo, Antonio O.T. Patrocinio, and Renata C. Lima. 2019. "Effect of Gd^{3+} Doping on Structural and Photocatalytic Properties of ZnO Obtained by Facile Microwave-hydrothermal Method." SN Applied Sciences 1 (4): 1–13. https://doi.org/10.1007/s42452-019-0359-x.

[7] Kasirajan, K., L. Bruno Chandrasekar, S. Maheswari, M. Karunakaran, and P. Shunmuga Sundaram. 2021. "A Comparative Study of Different Rare-Earth (Gd, Nd, and Sm) Metals Doped ZnO Thin Films and Its Room Temperature Ammonia Gas Sensor Activity: Synthesis, Characterization, and Investigation on the Impact of Dopant." Optical Materials 121 (September): 111554. https://doi.org/10.1016/j.optmat.2021.111554.

[8] Tawil, Siti Nooraya Mohd, D. Krishnamurthy, R. Kakimi, S. Emura, S. Hasegawa, and H. Asahi, 2011. "Studies on the InGaGdN/GaN Magnetic Semiconductor Heterostructures Grown by Plasma-assisted Molecular-beam Epitaxy." *Journal of Crystal Growth* 323(1): 351–54. http://dx.doi.org/10.1016/j.jcrysgro.2010.11.166.

[9] Tawil, Siti Nooraya Mohd, D. Krishnamurthy, R. Kakimi, S. Emura, S. Hasegawa, and H. Asahi, 2011. "Influence of Si-Doping on the Characteristics of InGaGdN/GaN MQWs Grown by MBE." *Physica Status Solidi (C) Current Topics in Solid State Physics* 8(2): 491–93.

[10] Ipek, Yeliz, and Nagihan Karaman Ayhan. 2021. "Rare Earth Element Doped ZnO Thin Films." International Journal of Pure and Applied Sciences 7 (2): 305–13. https://doi.org/10.29132/ijpas.944792

[11] Ba[illegible] V. 201[illegible]. "[illegible] A Review of Applications, Occurrence, Exploration, Ana[illegible], R[illegible]ycling, [illegible] Envi[illegible]ment[illegible] Impact." Geoscience Frontiers 10 (4): 1285–1303. htt[illegible]/[illegible]g/10.10[illegible]/j.gsf.2018.12.[illegible]5.

[12] Maz[illegible], [illegible] and M[illegible] Tafre[illegible] 2018. "The Effects of Gadolinium Doping on the Structural, Morphological, Optical, and Photoluminescence Properties of Zinc Oxide Nanoparticles Prepared by Co-Precipitation Method." Applied Physics A: Materials Science and Processing 124 (12), 0[illegible] [illegible]ttps://[illegible]org/10.1007/s00339-018 2291-0.

[13] Anand, [illegible], [illegible] Sakthiv[illegible], K. [illegible] Arun Kumar, S. Valanarasu, V. Ganesh, Mohd Shkir, A. Kathalin[illegible] and S. AlFaif[illegible] 2019. "Novel Rare Earth Gd and Al Co-Doped ZnO Thin Films Prepared by Nebulizer Spray Method for Optoelectronic Applications." Superlattices and Microst[illegible]uctures 123 (August): 311–22. [illegible]ttps://doi.org/10.1016/j.spmi.2018.09.014.

[14] El F[illegible], [illegible] V[illegible] Torc[illegible], [illegible] Rodríg[illegible], G. Polupan, and J. Douda. 2024. "Impact of A[illegible] a[illegible] Co-D[illegible]ping on Transmittance, Band Gap Energy, and Electrical Characteristics of ZnO [illegible] T[illegible] A[illegible]" Journal of Materials Science: Materials in Electronics 35(16): 1–6 [illegible]ttps://doi.org/10.1007/[illegible]-024-12773-[illegible].

[15] Tsay, C[illegible]en [illegible]e, and S[illegible]h Hsu[illegible] Y[illegible] 202[illegible]. "Me[illegible]ation of Electrical and Optical Properties of Al [illegible] and [illegible] Co-Doped ZnO [illegible]sparent Semi[illegible]ductor Thin Films." Coatings 11 (10). htt[illegible]//doi.org/10.3390/coatings11101259.

[16] Toma, M., [illegible] Marcon[illegible], Mari[illegible]a Pop, C. Lung, and A. Pop. 2019. "Influence of Substrate-Target Distance on Structural and Optical Properties of Ga and (Al + Ga)-Doped ZnO Thin Films Deposited by Radio Frequency Sputtering." *Analytical Letters* 52 (14): 2227–38. htt[illegible]//doi.org/10.10[illegible]/00032719.201[illegible].160681

[17] Liu, [illegible]a[illegible], and [illegible]min[illegible] Zhu. 2019. "Preparation and Characterization of Mg, Al and Ga Co-Doped ZnO Transparent Conductive Films Deposited by Magnetron Sputtering." Results in Physics 14(April): 102514. https://doi.org/10.1016/j.rinp.2019.102514.

[18] Sun, H[illegible], S[illegible] Chi Chen, [illegible] Hsien Wang, Yu Wei Lin, Chao Kuang Wen, Tung Han Chuang, X[illegible] W[illegible], [illegible] and Ming [illegible] Dai. 2019. "Electrical and Magnetic Prop[illegible] (Al, Co) Co-Doped ZnO F[illegible] Depo[illegible]ted by RF Magnetron Sputtering." Surface and [illegible]atings Technology 359 (August 2018): 390–95. http[illegible]//doi.org/10.1016/j.surfcoat.2018.10.105.

[19] Winarsi[illegible], S[illegible], [illegible] R[illegible]dina, and [illegible] Watanabe. 2024. "Effect of Cobalt and Alumin[illegible] [illegible] Magnetic Properties of Zinc Oxide Nanoparticles." AIP A[illegible] 14(4). [illegible]/5.0[illegible]1075

[20] Khan, [illegible] and Wei Guo Huang. 2024. "Induced Fer[illegible] via Al Co-Doping and Their Optical Charac[illegible] (20).

[21] Figi[illegible] 2021. "Journal of Alloys and Compounds: Preface [illegible] Alloys and Compounds 404–406 (SPEC. ISS.): 1. https://doi.org/10.10[illegible]/j.jallcom.2005.05.002.

[22] Khan, Rajwali, [illegible] Otaibi, Khaled Althubeiti, Sherzod Shukhratovich Abdullaev, [illegible] Muhammad [illegible] Aurangzeb Khan, Shahid Iqbal, Tommaso Del Ross[illegible] and A[illegible] Khan. 2022. "Room Temperature Dilute Magnetic Semiconductor Response in (Gd, Co) Co-Doped ZnO for Efficient Spintronics Applications." RSC Advances 12 (55): 36126–37.

[23] Selvaraj, Saravanan, V. Krishna Mohan, M. Navaneethan, S. Ponnusamy, and C. Muthamizhchelvan. 2019. "Synthesis and Photocatalytic Activity of Gd Doped ZnO Nanoparticles [illegible] of Methylene Blue under Visible Light." Materials

Science [illegible] Processing 103 (July): 104622. https://[illegible]10.10[illegible]2019.104622.

[24] Ba[illegible] Veyse[illegible] 2019. "Optical, Structural and Phase Tra[illegible] Their Photoelectrochemical Sensor App[illegible] International Journal of Hydrogen Energy 18744–55.

[25] Tawi, S. N. M., C. A. [illegible], N. Sarip, S. A. Kamaruddin, A. R. Nurulfadzilah, A. Miskon, and M. Z. Sa[illegible]. 20[illegible] "Effect of Rare-Earth Gd Incorporation on the Characteristics of ZnO Thin [illegible] Journal of Nanoscience and Nanotechnology 15 (11): 9212–16. https://[illegible]

[26] Bhar[illegible] M. Navaneethan, J. Archana, M. Ganesh Kumar, et al. 2020. "Growth and Influence [illegible] Gd Doping on ZnO Nanostructures for Enhanced Optical, Structural Properties and Gas Sensing Applications." Applied Surface Science [illegible] https://doi.org/10.1016/j.apsusc.2019.143857.

[27] Taw[illegible] Krishnamurthy, Shuichi Emura, [illegible] 2010. "Characterization of InGaGdN Layers [illegible]" Physica Status Solidi - Rapid Research Letters 4 (11): [illegible] https://doi.org/10.1002/[illegible]2010[illegible]73.

[28] Rashid, Nur Amaliyana [illegible], Mohd Tawi, and Nafarizal Nayan. 2023. "Effect of Al Concentration [illegible] Properties of (Ga, Al) Co-Doped ZnO and Its [illegible] Structures Prepared via Co-Sputtering Method." Materia[illegible] 2392. https://doi.org/10.3390/ma16062392.

[29] Safee[illegible], Akif [illegible], Danish Arif, Wiqar H. Shah, Akhtar Ali, Ghafar Ali, Fayaz Hussain. 2023 "Tuning the Optical Properties of ZnO by Co and Gd Doping for Water Pollutant Elimination." Water [illegible] https://doi.org/10.3390/w15081470.

[30] Assim, [illegible] and Optical Properties of Nanopowders CdS: XAl (X=0, 1[illegible]) [illegible] Technique." Egyptian Journal of Solids 43(1): 111–25.

[31] Muktaridha Omar, Muhammad Adlim, Surya[illegible] Suhendrayatna, and Ismail Ismail. 2021 [illegible] Nanoparticles and the Photocatalytic Properties. [illegible] Chemistry 14(6): 103175. https://[illegible]3175.

[32] Wang, [illegible] 2021. "Preparation and Characterization of (A[illegible] Films Prepared by Sol–Gel." Coatings 11(8).

[33] Po[illegible] P. T. Poojitha, and Si Hyun Park. 2017 [illegible] by Al Co-Doping." Journal of Alloys [illegible] https://doi.org/10.1016/j.jallcom.2017.01.328.

[34] Arm[illegible] "Role of Gd^{3+} and Ho^{3+} Doping on the Structur[illegible] Applied Physics A: Materials Science and [illegible]10.1007/s00339-023-06569-2.

[35] Com[illegible] Emission in Ultrawide Bandgap Semicon[illegible]structures." *Advanced Optical Materials* 11(1).

[36] Yidong [illegible] 2019. "Preparation and Magnetic Properties of Fe Doped ZnO Thin Films with Dilute Magnetic Semiconductors." International Journal of Nanoparticles and Na[illegible] https://doi.org/10.35840/2631-5084/5528.

[37] Dev[illegible] 20[illegible] "Theory of Magnetic Domain Phases in Ferro[illegible]" *Physical Review Letters* 12[illegible] (11): 117002.

[38] Agarw[illegible], Fouran Singh, A Tripathi,

Jiten[illegible] Singh, [illegible] Avasthi. 2019. "Enhanced Room Temperature Ferromagnetism and Band Gap Tuning in Ga Doped ZnO Thin Film Synthesised by Neutral Beam Sputtering." Scientific Reports 9 (1): 6675. https://doi.org/10.1038/s41598-019-43149.

[39] Jin, Yunlong, Lanping Yue, and David J. Selmyer. 2017. "Effect of In-Situ Annealing Temperature on Magnetic Domain Structure and Magnetism of Zr_2Co_{11} Thin Films." Thin Solid Films [illegible] (2017): [illegible], 10.1016/j.tsf.2017.08.018.